

Maximal Cliques on Multi-Frame Proposal Graph for Unsupervised Video Object Segmentation

Jialin Yuan ^{*}
Oregon State University
yuanjial@oregonstate.edu

Jay Patravali ^{*}
Oregon State University
patravaj@oregonstate.edu

Hung Nguyen
Oregon State University
nguyehu5@oregonstate.edu

Chanho Kim
Oregon State University
kimchanh@oregonstate.edu

Li Fuxin
Oregon State University
lif@oregonstate.edu

Abstract

Unsupervised Video Object Segmentation (UVOS) aims at discovering objects and tracking them through videos. For accurate UVOS, we observe if one can locate precise segment proposals on key frames, subsequent processes are much simpler. Hence, we propose to reason about key frame proposals using a graph built with the object probability masks initially generated from multiple frames around the key frame and then propagated to the key frame. On this graph, we compute maximal cliques, with each clique representing one candidate object. By making multiple proposals in the clique to vote for the key frame proposal, we obtain refined key frame proposals that could be better than any of the single-frame proposals. A semi-supervised VOS algorithm subsequently tracks these key frame proposals to the entire video. Our algorithm is modular and hence can be used with any instance segmentation and semi-supervised VOS algorithm. We achieve state-of-the-art performance on the DAVIS-2017 validation and test-dev dataset. On the related problem of video instance segmentation, our method shows competitive performance with the previous best algorithm that requires joint training with the VOS algorithm.

1. Introduction

For robots to operate safely and reliably in dynamic environments or ‘in-the-wild’, they must be able to discover novel unseen objects with no supervision from continuous video streams. Robots can be pre-trained to understand what general objects may look like, but once deployed in the field, it would be very difficult to supply them with additional annotations. It is especially likely that objects from

novel categories unseen from the training set would need to be discovered. Hence, acquiring this capability of unsupervised object discovery from new videos, which more commonly is called Unsupervised Video Object Segmentation (UVOS) [6], is an important research problem.

In the related problem of semi-supervised Video Object Segmentation (VOS), the first frame annotation is provided to the algorithm, which tracks and segments each object throughout the rest of the video. Most recent works typically utilize space-time transformers like STM [35] which properly match the visual features in a new frame with previous frames using a deformable attention model. This helps the systems track objects across significant motion, deformation, and occlusion.

Hence, a simple and natural idea to address the UVOS problem in prior work is to identify object proposals on a few key frames and then utilize a semi-supervised VOS algorithm to track them [31]. Usually, instance segmentation algorithms such as Mask-RCNN [21] are utilized to identify object proposals in those key frames. However, for VOS to work well, the starting frame usually needs to be annotated with high precision, because wrongly annotated regions in this frame, serving as ground truth, could lead to significant drift in subsequent frames. Similarly, a missing part from the annotation might be missed forever because the tracker thinks it belongs to the background instead of the object. Hence, achieving high segmentation accuracy at those key frames is essential for better UVOS performance.

However, single-frame instance segmentation is often noisy and does not always provide the required precision in the key frames. In this paper, we present a novel approach to improve the segmentation on the key frames. The idea is to take into account object proposals from nearby frames and use them to jointly reason about the segmentation in the key frame, which allows segmentations from different frames to cancel out the noise in each other.

^{*} Equal contributions.

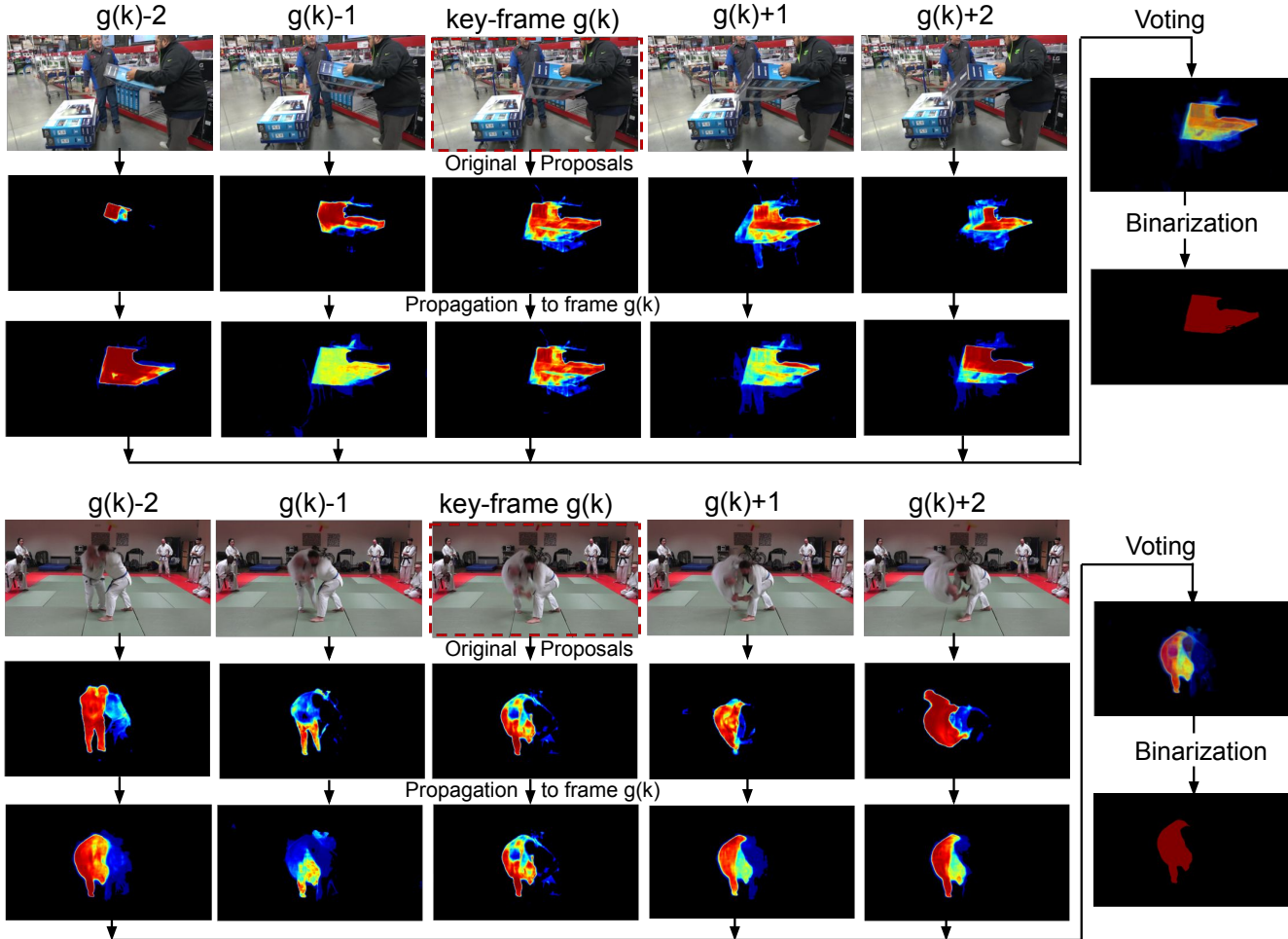


Figure 1. Illustration of the proposed MCMPG for object proposal refinement using a key frame clip with size 5 (“loading” and “judo” from DAVIS 2017 val set). **On the left side:** the first row are the RGB frames within the local window (the key frame $g(k)$ is the central frame highlighted in the red border). The second row is the segmentation of the object (the package box in “loading”, the left person in “judo”) on each frame. The third row shows the proposals propagated to the key frame. **On the right side:** the first image is the voting of the object proposals inside a maximal clique on the *MP-Graph*, which is created with all propagated object proposals initially generated on the key frame clip. The second image is the final binarized object mask we obtained.

Our approach builds a **Multi-frame Proposal Graph** (MP-Graph) using object proposals initially generated in a local window around each key frame, and then locates maximal cliques in this graph from which the final segmentation on the key frame is generated. Each clique in the graph consists of multiple segments that correspond to the same object, hence jointly reasoning among all of them may generate more precise segmentations. Fig. 1 shows two examples, where the segmentation of the object is poor on the key frame, meanwhile, none of the segmentations from the five frames are perfect. However, their joint voting produces a segmentation very close to the ground truth. Once better key frame segmentation is obtained, we can use any VOS algorithm to propagate it to the entire video and use a sequence non-maximum suppression (NMS) approach to filter out redundant objects. Our approach is lightweight

and fast, and thus adds little computational overhead to the VOS algorithms used for tracking key frame proposals. Although our approach does not handle instance classification, we also extend our approach to a similar problem of Video Instance Segmentation (VIS), where it is required to classify the tracked object instances to a known set of categories, extending image instance segmentation to the video domain.

We validate our approach through extensive experiments providing quantitative and qualitative analysis on both tasks. Experiments on the DAVIS-UVOS and Youtube-VIS benchmark show that the better key frame segmentations from our approach lead to state-of-the-art performance. Notably, our approach outperforms the state-of-the-art [26] in UVOS that jointly trains the proposal generation model and the STM model. Not needing joint training is a significant advantage of our model – this makes it future-proof because

it can be then plugged in seamlessly to any future VOS models that achieve better performance without a cumbersome re-training process.

To summarize, our main contributions are,

1. We propose **Maximal Cliques on Multi-Frame Proposal Graph (MCMPG)**, which utilizes maximal cliques over a graph of object proposals from a local window. Reasoning over the multiple similar proposals within these maximal cliques over this graph yields better object proposals. MCMPG is *modular*, *lightweight*, and *fast*, enabling it to be plugged into any VOS algorithms that track object proposals without requiring the joint training that previous methods need.
2. MCMPG outperforms all SOTA unsupervised methods on the DAVIS-UVOS validation and test-dev set. Furthermore, it significantly improves the performance given the same single-image instance segmentations in the Video Instance Segmentation Task on the Youtube-VIS 2019 validation set benchmark.

2. Related Work

Image Instance Segmentation. The task is to produce pixel-level predictions for each object instance in a frame. Top-down [21, 22, 29] approaches like Mask-RCNN [21] and its follow-ups adopt the ‘detect-then-segment’ paradigm. These two-stage approaches are accurate but relatively slow due to the exhaustive search process.

To overcome these drawbacks, bottom-up methods [15, 28, 32] view the problem as ‘label-then-cluster’ where the model learns an affinity function to group pixel embeddings belonging to the same object instance. Single-stage algorithms [50, 51, 58, 61] simplify computational-heavy post-processing, and in particular, SOLO [50] and SOLOv2 [51] segment the object instances by locations without using bounding boxes or metric learning. DETR [8] inspires End-to-End transformer-based models [10, 11, 16, 41, 46]. The most recent Mask2Former [10] uses masked attention to achieve state-of-the-art performance in the instance segmentation task.

Semi-Supervised Video Object Segmentation. Video Object Segmentation (VOS) can be applied to acquire pixel-level segmentations of primary objects in the scene given unconstrained videos. Depending on the level of supervision, they can be categorized as semi-supervised (one-shot), interactive, and unsupervised (zero-shot). Early work [5, 13, 36] fine-tuned a pretrained network at test-time using multiple data augmentations on the mask of each object from the first frame. They are usually very slow due to the excessive test-time fine-tuning. Their performance under occlusion and appearance changes is also limited due to the overfitting to the appearance of the first frame.

Later approaches improved speed and accuracy through metric learning [9, 45], guided propagation [34, 35, 60] and transformer-type networks [12, 25, 33, 35, 39, 55].

Unsupervised Video Object Segmentation. Early work utilizes motion patterns such as clustering object motion trajectories [4, 17, 57] or deep CNN-based spatio-temporal grouping [14, 57]. Some combine appearance with optical flow for enhanced object features [13, 30, 63], or use optical flow alone [43]. A common drawback to these methods lies in their inability to be generalized to videos that have static objects, large motion blur, or cluttered backgrounds.

For multi-object VOS, learning appearance models of all the object proposals have been previously explored [24, 56]. Currently, ‘track-by-detect’ [18, 31, 31, 44, 48] paradigm is popular where instance segmentation framework generates object proposals via Mask-RCNN [21] which then are tracked consistently through a video sequence. UnOVOST [31] pruned tracklets from proposals into long-term tracks via visual similarity. In AGNN [48], mask proposals over a video sequence were aggregated via graph neural networks. Most recently, [62] proposed a novel instance segmentation, tracking, and re-identification network.

Video Instance Segmentation. The VIS task was proposed in MaskTrack R-CNN [59] which adds a tracking head to Mask RCNN and an external memory to store and associate features of object instances across multiple frames. This tracking paradigm is extended in [2, 7] and STEMseg [1] models video clips as 3D space-time volumes to predict masks by clustering learned embeddings. An application of graph neural networks is seen in Vis-STG [47]. Propose-Reduce [26] generates instance sequence proposals on key frames and reduces redundant sequences of the same instances with non-maximum suppression. Transformer-based techniques have become increasingly successful [23, 42, 52, 53] applying cross-attention to process video clips. Mask2Former is extended to VIS [10] by directly making predictions on the entire video sequence. Online VIS methods also exist, but they usually have lower accuracy due to not observing the entire sequence [20, 54].

3. Proposed Method

The architecture of using MCMPG to perform UVOS is shown in Fig. 2. MCMPG aims to generate the key frame proposals with higher quality by creating a multi-frame proposal graph and finding its maximal cliques. Afterward, any semi-supervised VOS algorithm can be used to track each instance proposal to the beginning and end of the sequence. Lastly, we adopt sequence NMS in order to remove duplicate segments.

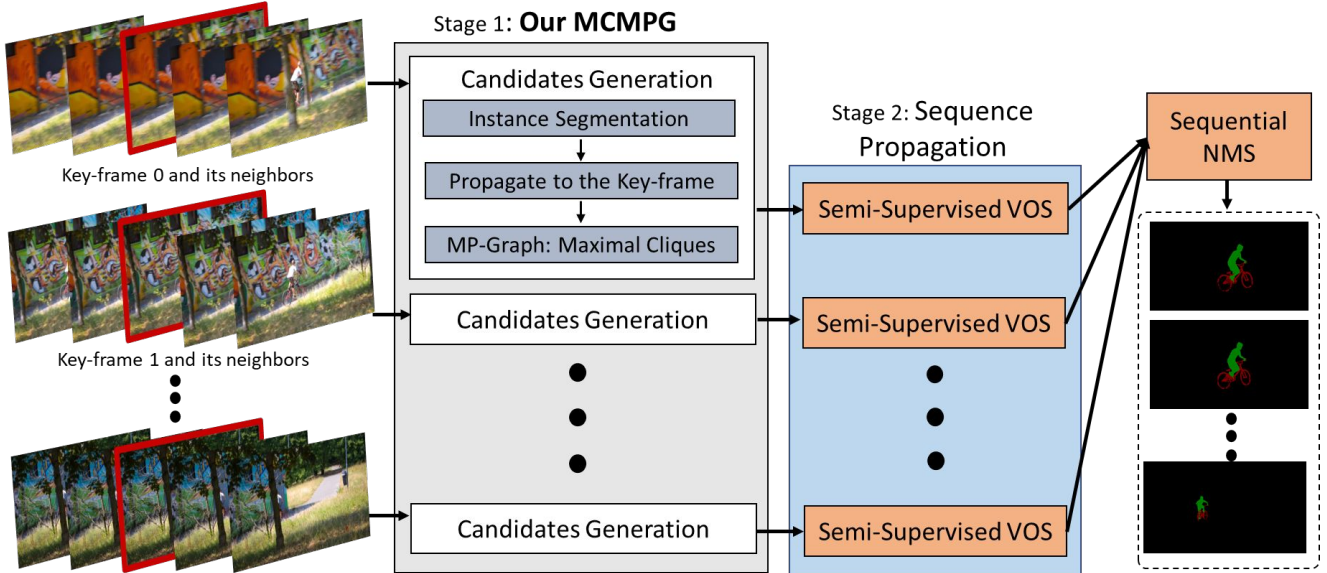


Figure 2. Architecture of the proposed MCMPG algorithm for the UVOS task. It includes 2 stages: (1) MCMPG: key frame proposals are generated from each *key frame clip*, including the key frame and its neighboring frames; (2) a tracker tracks these proposals bidirectionally through the whole sequence to obtain the final unsupervised video object segmentation. Our main contribution MCMPG includes 3 steps: 1) Run instance segmentation on each frame in the key frame clip; 2) Propagate the proposals to the key frame; 3) Create the *MP-Graph* from the propagated proposals and locate its maximal cliques. By combining proposals within these maximal cliques, we can obtain object proposals that are better than the instance segmentation result of any frame and subsequently improve the performance of the UVOS task. (Best viewed in color)

3.1. Problem Definition

Given a set of RGB frames $\mathcal{I} = \{I_t\}_{t=0}^{T-1}$ where $I_t \in \mathcal{R}^{3 \times h \times w}$ and T is the total number of frames, the goal is to produce a sequence of consistent segmentation masks $\mathcal{S} = \{M_t\}_{t=0}^{T-1}$ for each of the m objects in the video. where $M_t \in \mathcal{R}^{m \times h \times w}$ represents the masks for all of the objects.

3.2. Proposal Generation on Key Frames

As we argued in the introduction, the quality of the generated key frame proposals is crucial for successful unsupervised video object segmentation. However, as Fig. 1 shows, even state-of-the-art instance segmentation approaches can generate bad segments in some frames due to motion blur, occlusion, and object poses that are very different from the training set. In this section, we introduce a new algorithm that improves key frame proposals by joint reasoning from many frames. The algorithm is illustrated in Alg. 1.

Key Frame Selection. Similar to [26], we select K key frames with fixed intervals. Namely, for a T -frame video, K frames $\{I_{g(0)}, \dots, I_{g(K-1)}\}$ are selected evenly starting from frame 0.

$$g(k) = k \max(\lfloor T/K \rfloor, 1), k = 0, \dots, K-1 \quad (1)$$

In contrast to [26] that uses the segments in the key frames directly as key frame proposals to track, we select a key frame clip to generate the key frame proposals. Here,

the key frame clip on a key frame $I_{g(k)}$ is $I_{g(k)}^C = \{I_i | i = g(k) - \frac{H-1}{2}, \dots, g(k) + \frac{H-1}{2}\}$. It contains the key frame itself and its $H-1$ neighbors from a local window centered around the key frame.

Instance Segmentation and Propagation. With the key frame clip $I_{g(k)}^C$, we first run image-level instance segmentation in each frame individually. Then we propagate all the segments S_i^I to the key frame $g(k)$ by using the same tracking algorithm that we use in the later stage (Stage 2 in Fig. 2). The set of propagated proposals is denoted as $S^{g(k)} = \{S_i^{g(k)} | i = g(k) - \frac{H-1}{2}, \dots, g(k) + \frac{H-1}{2}\}$, where $S_i^{g(k)} \in \mathcal{R}^{L_i \times h \times w}$ is the probability masks of L_i proposals that are segmented in frame i and then propagated to the key frame $g(k)$. This set can be used to create the multi-frame proposal graph which is introduced below.

MP-Graph (Multi-frame Proposal Graph). On the proposal set $S^{g(k)}$ from one key frame clip, we create an undirected graph where each propagated proposal in $S^{g(k)}$ is one vertex in the graph, and an edge is created between a pair of vertices if their Intersection-over-Union (IoU), Eq.(2) is larger than t_0 .

$$IoU(S_{i,o_1}^{g(k)}, S_{j,o_2}^{g(k)}) = \frac{S_{i,o_1}^{g(k)} \cap S_{j,o_2}^{g(k)}}{S_{i,o_1}^{g(k)} \cup S_{j,o_2}^{g(k)}} \quad (2)$$

where $S_{i,o_1}^{g(k)}, S_{j,o_2}^{g(k)}$ are two propagated proposals from the

temporal frame i and j to the key frame $g(k)$ so that their IoU is measured in the same key frame.

Algorithm 1: Key frame Proposal Generation

Input : key frame and its neighbours
 $\{I_i | i = g(k) - \frac{H}{2}, \dots, I_{g(k) + \frac{H}{2}}\}$

Output: Instance Proposals S in the key frame

- 1 **for** $i \leftarrow g(k) - \frac{H}{2}$ **to** $g(k) + \frac{H}{2}$ **do**
- 2 | $S_i^I \leftarrow \text{InstanceSegmentation}(I_i)$
- 2 | $S_i^{g(k)} \leftarrow \text{Propagate}(S_i, \{I_i \dots I_{g(k)}\})$
- 3 **end for**
- 4 $G = \text{MP-Graph}(S^{g(k)})$
- 4 | $\text{Cliques} = G.\text{maximalCliques}()$
- 5 **for** $C \in \text{Cliques}$ **do**
- 6 | $S^c \leftarrow \text{combine}(C, S^{g(k)})$ // Eq. 3
- 7 **end for**
- 8 $S_k \leftarrow \cup S^c$
- 9 **return** S_k

We name the graph as the Multi-frame Proposal Graph given that its nodes are propagated proposals from different temporal frames and its edges are created based on the spatial IoU computed in the same time frame $g(k)$. After the *MP-Graph* is created, we adopt the *maximal clique algorithm* [3] to generate the final instance proposals in the key frame to be tracked (See Fig. 3).

Key Frame Proposals. In an undirected graph, a *clique* is a complete sub-graph in which every two vertices are adjacent. A *maximal clique* is a clique that *cannot be extended* by including *any more adjacent* vertex. The largest maximal clique is called a *maximum clique*. Accordingly, in the *MP-Graph*, a *maximal clique* is a subset of propagated proposals which all significantly overlap each other.

Given a maximal clique C that contains n propagated proposals $\{O_i | i = 0, \dots, n-1\}$, $n \leq H$, its corresponding key frame object proposal S^C is computed as:

$$S^C = \left(\frac{1}{H} \sum_{i=0, \dots, n-1} O_i \right) \geq t_1 \quad (3)$$

where t_1 is a threshold that can be set to a small value (0.2 in the experiments) without introducing noise in the segmentation. In the "loading" example in Fig.1, the propagated proposals from $g(k) - 2$, $g(k)$, and $g(k) + 2$ have low confidence on the bottom left part of the package box object and high confidence on the right corner, while the propagated proposal from $g(k - 2)$ has high confidence on the bottom left part and has low confidence on the right corner. Thus, the maximal clique including the proposals propagated from $g(k) - 2$, $g(k) - 1$, $g(k)$, and $g(k) + 2$ can smooth the score over the object and then segment the package correctly. Notably, the algorithm can retrieve the object proposals even

when the segmentation on the key frame is poor. In the "judo" example presented in Fig.1, the segments of the person on the left are noisy in the first three frames due to serious motion blur, but the final, combined proposal for the person in the clique consisting of propagated proposals from frame $g(k) - 2$, $g(k) + 1$, and $g(k) + 2$, is a better segmentation result due to predictions in the last two frames that fill in the missing pixels and remove the false pixels.

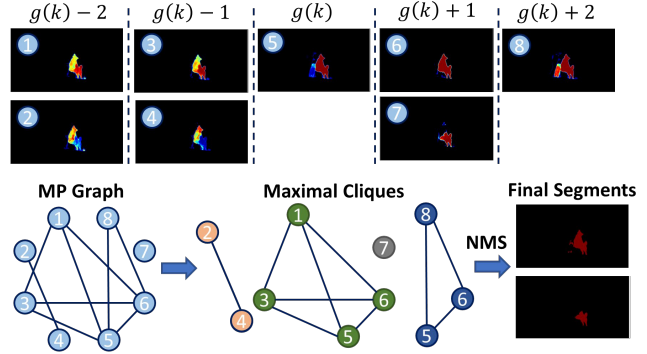


Figure 3. An example of Multi-frame Proposal Graph. Propagated segments are connected based on their IoU on the key frame, then one segment is generated from each clique (Best viewed in color)

3.3. Tracking

Sequence propagation. After the key frame proposals are obtained, an off-the-shelf semi-supervised VOS method can be used to track all the objects from the key frame bidirectionally through the video sequence. In this way, we can always plug in state-of-the-art VOS algorithms for better performance. The propagation results from each key frame $\{S_k | k = 0, \dots, K - 1\}$ are then concatenated together as $\hat{S} \in \mathcal{R}^{T \times N \times h \times w}$, assuming we segment N objects in total after the tracking stage.

Sequence Score. We compute the score of an object sequence \hat{S}_o by referring to the object masks S^I and objectness scores C^I obtained from the instance segmentation model. The sequence score is then computed by

$$\text{Score}_o = \frac{1}{T} \sum_{t=0, \dots, T-1} \max_i (\text{IoU}(\hat{S}_o^t, S_i^I) C_i^I). \quad (4)$$

where i iterates over the object proposals from the instance segmentation on frame t . We utilize the objectness scores C_i^I from the instance segmentation model without re-computing the objectness of the new object masks coming from tracking. This avoids re-running the objectness computation for the merged mask. The sequence score for each object sequence is used in Sequence NMS for removing duplicate object sequences that are detected in different key frames. It is also used to rank object sequences in the case where the algorithm is allowed to output only a fixed number of detections. Our sequence NMS follows [26] which

removes overlapping tracks by running the traditional NMS algorithm with the tracking scores and the sequence IoU.

4. Experiments

4.1. Implementation Details

Architecture. Our proposed architecture is shown in Fig. 2. K key frames are sampled from a given video sequence and the corresponding key frame clips are fed to a network to obtain image-level object segmentation proposals. Then the second network is utilized to propagate the initial segments to their related key frames. Afterwards, the *MP-Graph* is built to compute the maximal cliques. Each maximal clique generates one key frame proposal by averaging over the propagated proposals in the clique and then binarizing with t_1 . The key frame proposals with areas smaller than 10 pixels are discarded. Finally, the second network is used again to track these key frame proposals to the beginning and end of the video.

This architecture is modular, so it is easy to replace both the instance segmentation and tracking methods with state-of-the-art algorithms. The methods we adopted for DAVIS and Youtube-VIS are discussed in Sec. 4.2 and Sec. 4.3 respectively.

Training / Inference. With pre-trained models for instance segmentation and semi-supervised VOS network, our approach does not need extra training. In our experiments (except ablations), the number of key frames K is set to 2 on DAVIS and 8 on Youtube-VIS, the size of key frame clip $H = 3$, threshold $t_0 = 0.5, t_1 = 0.2$.

4.2. Unsupervised Video Object Segmentation

Dataset. The DAVIS 2017 [38] benchmark is used for video multi-object segmentation with high-quality masks for salient objects. It consists of 60 sequences used for training and 30 for validation. DAVIS 2019 [6] is an extension of DAVIS 2017 for the UVOS task. It has the same training and validation set as DAVIS 2017 and 30 new sequences in its *test-dev* set. To demonstrate that our proposed *MP-Graph* is network-agnostic and can work with a wide range of instance segmentation models, we show experimental results with both SOLOv2 [51] and Mask-RCNN instance segmentations from [26]. SOLOv2 model is initialized with COCO pretrained weights. We then fine-tune its kernel branch and feature branch for 10 epochs, then the FPN for 5 epochs, and finally the ResNet-101 backbone blocks from the last block to the first block for 5 epochs per block. Similarly, for the tracker, we show experimental results with both STM [35] and STCN [12].

Metric. We follow the standard evaluation settings [37]: the performance is reported in terms of region similarity \mathcal{J} , boundary accuracy \mathcal{F} , and the overall metric $\mathcal{J}\&\mathcal{F}$. The evaluation scores on the *test-dev* set are obtained from the

evaluation server of the DAVIS 2019 challenge.

Results on DAVIS 2017 *val*. In Table 1, we compare our approach with state-of-the-art unsupervised video multi-object segmentation methods on the DAVIS 2017 dataset. The common baselines from published works are included: RVOS [44], PDB [40], AGS [49], ALBA [49], MATNet [63], AGNN [48], and Stem-Seg [1]. Some of the recent top-ranked methods include UnOVOST [31], Target-Aware [62], and Propose-Reduce [26]. As shown in Table 1, on DAVIS 2017 *val*, our approach achieves the highest overall results across most metrics. Prior methods such as UnOVOST and MATNet are computationally expensive and also need to compute optical flow for motion estimation. Our work requires only RGB frames as input and outperforms the previous best method Propose-Reduce [26] by 1.7% in terms of \mathcal{J} & \mathcal{F} -Mean when using the same instance segmentation method and the same ResNeXt-101 backbone. With the more complex ResNeXt-101 backbone, we outperform [26] by 7.8%. Note that by utilizing frames next to the key frames, our approach may be thought of as utilizing more frames than [26]. However, the ablation study in [26] shows that more key frames do not further help their performance on this dataset, which shows the importance of MCMPG in terms of combining and refining the proposals.

In Table 1, we also adopt the Mask-RCNN module from [26] to compute the key frame proposals. This approach without the *MP-Graph* achieves a score 1.7% higher than [26] since we adopt a separate STM model to perform tracking. Adding *MP-Graph* improves another 1.7% over this baseline, which shows the effectiveness of MCMPG even with the same object proposal algorithm as [26]. The modular design of the proposed framework also makes it easy for a different tracking algorithm to be plugged in without joint training. In order to show this, we report the performance of MCMPG with STCN [12] as well.

Results on DAVIS 2019 *test-dev*. We evaluate the proposed approach MCMPG on DAVIS 2019 *test-dev* set shown in Table 2. Our approach achieves the state-of-the-art result in terms of \mathcal{J} & \mathcal{F} -Mean at 61.2. Compared with the previous state-of-the-art Target-Aware [62], our approach improves significantly on the boundary F-metric, which shows that our proposals cover object boundaries significantly better. Here we do not test the ResNeXt-101 backbone for a fair comparison with prior work, which also does not use this more complex backbone.

4.3. Video Instance Segmentation

Video Instance Segmentation (VIS). Different from UVOS which segments salient object instances, VIS aims at discovering and segmenting all object instances of pre-defined object categories from videos. It requires predictions for both object segmentations and object categories.

Table 1. Quantitative video multi-object segmentation results on DAVIS 2017 *val*.

Methods	Instance Seg.	backbone	\mathcal{J} & \mathcal{F} Mean	\mathcal{J} -Mean	\mathcal{J} - Recall	\mathcal{J} - Decay	\mathcal{F} -Mean	\mathcal{F} - Recall	\mathcal{F} - Decay
RVOS [44]	-	ResNet-101	41.2	36.8	40.2	0.5	45.7	46.4	1.7
PDB [40]	-	ResNet-50	55.1	53.2	58.9	4.9	57.0	60.2	6.8
AGS [49]	-	ResNet-101	57.5	55.5	61.6	7.0	59.5	62.8	9.0
ALBA [19]	-	ResNet-101	58.4	56.6	63.4	7.7	60.2	63.1	7.9
MATNet [63]	-	ResNet-101	58.6	56.7	65.2	-3.6	60.4	68.2	1.8
AGNN [48]	-	ResNet-101	61.1	58.9	65.7	11.7	63.2	67.1	1.2
STEm-Seg [1]	-	ResNet-101	64.7	61.5	70.4	-4.0	67.8	75.5	1.2
UnOVOST [31]	-	ResNet-101	67.9	66.4	76.4	-0.2	69.3	76.9	0.0
Target-Aware [62]	-	ResNet-101	65.0	63.7	71.9	6.9	66.2	73.1	9.4
Propose-Reduce [26]	Mask-RCNN	ResNet-101	68.3	65.0	-	-	71.6	-	-
Propose-Reduce [26]	Mask-RCNN	ResNeXt-101	70.6	67.2	-	-	73.9	-	-
MCMPG + STM (<i>w/o MP-Graph</i>)	Mask-RCNN	ResNeXt-101	70.0	67.1	73.0	-1.1	72.3	80.0	0.9
MCMPG + STM (<i>w/ MP-Graph</i>)	Mask-RCNN	ResNeXt-101	71.7	68.9	74.6	-4.9	75.8	83.2	-2.1
MCMPG + STCN (<i>w/o MP-Graph</i>)	Mask-RCNN	ResNet-101	73.6	70.2	77.5	-2.3	77.1	83.4	0.2
MCMPG + STCN (<i>w/ MP-Graph</i>)	Mask-RCNN	ResNet-101	76.8	73.8	81.9	-1.2	79.2	85.5	1.9
MCMPG + STM (<i>w/o MP-Graph</i>)	SOLOv2	ResNet-101	71.2	68.2	76.5	-2.2	74.0	81.2	0.9
MCMPG + STM (<i>w/ MP-Graph</i>)	SOLOv2	ResNet-101	72.5	69.0	77.3	-3	76.1	83.3	5.3
MCMPG + STM (<i>w/o MP-Graph</i>)	SOLOv2	ResNeXt-101	72.7	69.9	76.6	-3.7	75.5	82.7	-1.1
MCMPG + STM (<i>w/ MP-Graph</i>)	SOLOv2	ResNeXt-101	78.4	75.4	83.9	0.05	81.4	88.9	0.04

Table 2. Quantitative video multi-object segmentation results on DAVIS 2019 *test-dev*.

Methods	Backbone	\mathcal{J} & \mathcal{F} Mean	\mathcal{J} -Mean	\mathcal{J} - Recall	\mathcal{J} - Decay	\mathcal{F} -Mean	\mathcal{F} - Recall	\mathcal{F} - Decay
RVOS [44]	ResNet-101	22.5	17.7	16.2	1.6	27.3	24.8	1.8
PDB [40]	ResNet-50	40.4	37.7	42.6	4.0	43.0	44.6	3.7
AGS [49]	ResNet-101	45.6	42.1	48.5	2.6	49.0	51.5	2.6
UnOVOST [31]	ResNet-101	58.0	54.0	62.9	3.5	62.0	66.6	6.6
Target-Aware [62]	ResNet-101	59.8	56.0	65.1	7.8	63.7	68.4	11.0
MCMPG + STM (<i>w/MP-Graph</i>)	ResNet-101	61.2	56.1	63.5	-0.2	66.4	71.9	-0.5

Usual VIS approaches contain a category classification head to predict the category score.

We adapt MCMPG to the VIS domain by adopting the Mask-RCNN module from [26] to generate object segments and the category scores on each frame as different settings. Meanwhile, STM [35] is used to propagate object segments generated on frames in a key frame clip to the key frame and to track key frame proposals bidirectionally throughout the videos. We also test our approach to the task by utilizing the latest transformer-based method, Mask2Former-VIS from [10], as the instance segmentation network.

Dataset. YouTube-VIS 2019 [59] is a large-scale dataset for VIS with objects in multiple categories. It contains 2, 283 high-resolution YouTube videos for training and 302 for validation, covering 4,883 unique object instances out of 40 categories. We use this dataset to examine the performance of our model in more challenging scenarios.

Metrics. YouTube-VIS adopted the standard evaluation metrics in image instance segmentation, average precision (AP) and average recall (AR), to evaluate performance. It follows COCO evaluation [27] to compute AP by averaging it over multiple intersection-over-union (IoU) thresholds from 50% to 95% at step 5%.

Results on YouTube-VIS 2019 *val*. We compare our approach with state-of-the-art video VIS approaches on the YouTube-VIS 2019 benchmark. As shown in Table 3, our approach achieves consistent improvements with all different backbones and instance segmentation methods. Specifically, adding the *MP-Graph* achieves at least 1.0% higher over the baseline without the *MP-Graph*, which shows the

effectiveness of the MCMPG. Note that the results on the YouTube-VIS are significantly affected by the accuracy of the object categorization, which is orthogonal to our contribution to improving the key frame segmentation. Hence, our AP@50 is not necessarily the best, since this metric is mainly affected by classification accuracy, but our higher AP and higher AP@75 indicate better segmentation quality our approach achieves. Compared with SeqFormer [53], our AP is higher, but AP@50 and AP@75 are both slightly lower. This shows that we very likely have achieved significantly better performance in the AP regimes even higher than 75% IoU, greatly indicating the strong segmentation quality our approach provides.

4.4. Ablation studies

Key Frame Selection. In Table 4, we illustrate the effectiveness of MCMPG on combining and refining the proposals with different numbers of key frames in Table 4 on DAVIS 2017 *val*. Without *MP-Graph*, it reduces to the baseline approach similar to [26], and the results in the table are comparable to [26] as well. With *MP-Graph* ($H = 3$), better segments that are obtained from merging proposals in the same clique show to improve performance at every setting of key frames, which validates that the proposed approach provides significant performance improvement as discussed in the paper. Also, we observe that the performance is robust to different numbers of key frames and satisfactory with just 2 key frames, not requiring an excessive amount of key frames to obtain good performance on this dataset.

Table 3. Results on YouTube-VIS 2019 *val*.

Methods	Instance Seg.	backbone	AP	AP@50	AP@75	AR@1	AR@10
SipMask [7]	-	ResNet-50	33.7	54.1	35.8	35.4	40.1
STEm-Seg [1]	-	ResNet-101	34.6	55.8	37.9	34.4	41.6
Target-Aware [62]	-	ResNet-101	37.1	57.1	40.9	34.8	43.2
Propose-Reduce [26]	-	ResNet-101	43.8	65.5	47.4	43.0	53.2
Propose-Reduce [26]	-	ResNeXt-101	47.6	71.6	51.8	46.3	56.0
MCMPG (<i>w/o MP-Graph</i>)	Mask-RCNN	ResNet-101	43.4	64.4	48.9	45.0	57.1
MCMPG (<i>w MP-Graph</i>)	Mask-RCNN	ResNet-101	44.6	64.2	49.5	46.4	58.5
MCMPG (<i>w/o MP-Graph</i>)	Mask-RCNN	ResNeXt-101	47.4	70.6	52.3	47.5	60.0
MCMPG (<i>w MP-Graph</i>)	Mask-RCNN	ResNeXt-101	48.4	70.4	52.7	48.6	60.1
transformer-based methods							
SeqFormer [53]	-	ResNet-101	49.0	71.1	55.7	46.8	56.9
Mask2Former [10]	Mask2Former-VIS	ResNet-101	49.2	72.8	54.2	-	-
MCMPG(<i>w/o MP-Graph</i>)	Mask2Former-VIS	ResNet-101	48.5	65.7	53.0	43.7	54.0
MCMPG(<i>w MP-Graph</i>)	Mask2Former-VIS	ResNet-101	50.5	70.3	55.0	45.0	55.8

Table 4. Ablation Study on DAVIS 2017 *val* on the influence of the number of key frames for with (*w/*) and without (*w/o*) using *MP-Graph* to generate refined object proposals.

No. of key frames	\mathcal{J} & \mathcal{F} -Mean <i>w/o MP-Graph</i>	\mathcal{J} & \mathcal{F} -Mean <i>w/ MP-Graph H = 3</i>
1	68.1	69.0 (+0.9)
2	70.5	72.5 (+2.0)
3	69.7	72.0 (+2.3)
4	71.2	72.0 (+0.8)
5	70.8	72.4 (+1.6)

Object proposal quality with *MP-Graph*. Here we provide a comparison of the object proposals quality with and without the *MP-Graph* on the key frames evaluated against the ground truth objects on the DAVIS 2017 *val* set. *MP-Graph* improves the key frame proposals by 3.7% in terms of *mIoU* as shown in Table 5. This significant improvement in the quality of the key frame proposal is the main driver of the performance of our approach.

Table 5. Quality of the key frame proposals on DAVIS 2017 *val*.

	<i>w/ MP-Graph</i>	<i>w/o MP-Graph</i>
<i>mIoU</i> (%)	79.2	75.5

4.5. Run-Time Analysis.

We report the run-time of each module in MCMPG in Fig. 4. The results are generated by using an NVIDIA Tesla V100 GPU. It shows that the process of generating proposals and improving them with the *MP-Graph* is very lightweight and takes minimal time to run. The most time-consuming part of the system is the semi-supervised VOS module. The limitation of MCMPG is that the VOS module needs to track objects starting from multiple key frames. In the STM algorithm, the encoder takes the object mask as *in-*

put. Hence, with each new object mask, the backbone has to be run again, which is quite suboptimal, especially for our approach which requires running tracking on a significantly larger amount of proposals than the regular semi-supervised VOS task for which STM was designed.

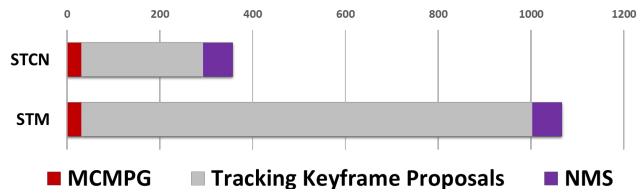


Figure 4. Run-time (in seconds) of MCMPG on DAVIS-UVOS 2017 *val* with 2 key frames. Note that MCMPG is fast (only 8.7% or 2.9% of the running time for STCN and STM VOS models, respectively), while improving the final tracking performance significantly. The bottleneck of the speed comes from an external tracking algorithm such as STM which requires re-running the backbone network for each proposal. Alternatively, one could use a newer tracking algorithm such as STCN where all the proposals can share the same backbone features, which would make the system much faster.

STCN [12] proposed to replace the memory encoder in STM with a lightweight encoder that does not require the mask as input. This improved both the speed and performance on the VOS task. For us, it implied that we would only need to run the encoder once. Thus, the speed of our system will be significantly faster without compromising performance if the system utilizes a STCN-type encoder, which we believe will be standard in the future. In Fig. 4, running VOS with STCN turns out to be at least 2.2× faster for us than STM.

5. Conclusion

To generate better key frame proposals in unsupervised video multi-video object segmentation, we introduce a

novel algorithm that aggregates object proposals in a local window to correlate space-time information in a graph. Maximal Cliques in this graph vote to eliminate false detections and ensure robust and accurate propagation of object proposals through a video sequence. With qualitative and quantitative experiments and analysis, we demonstrate that the mask proposal refinement provides significant performance improvements over state-of-the-art methods in the DAVIS-UVOS and Youtube-VIS benchmarks across different backbones and instance segmentation algorithms. In the future, we would like to pursue applications of this algorithm in realistic object discovery tasks, such as in robotics and autonomous driving applications.

References

- [1] Ali Athar, Sabarinath Mahadevan, Aljosa Osep, Laura Leal-Taixé, and Bastian Leibe. Stem-seg: Spatio-temporal embeddings for instance segmentation in videos. In *European Conference on Computer Vision*, pages 158–177. Springer, 2020. [3](#), [6](#), [7](#), [8](#)
- [2] Gedas Bertasius and Lorenzo Torresani. Classifying, segmenting, and tracking object instances in video with mask propagation. In *Proceedings of the IEEE/CVF Conference on Computer Vision and Pattern Recognition*, pages 9739–9748, 2020. [3](#)
- [3] Coen Bron and Joep Kerbosch. Algorithm 457: finding all cliques of an undirected graph. *Communications of the ACM*, 16(9):575–577, 1973. [5](#)
- [4] Thomas Brox and Jitendra Malik. Object segmentation by long term analysis of point trajectories. In *European conference on computer vision*, pages 282–295. Springer, 2010. [3](#)
- [5] S. Caelles, K.K. Maninis, J. Pont-Tuset, L. Leal-Taixé, D. Cremers, and L. Van Gool. One-shot video object segmentation. In *Computer Vision and Pattern Recognition (CVPR)*, 2017. [3](#)
- [6] Sergi Caelles, Jordi Pont-Tuset, Federico Perazzi, Alberto Montes, Kevis-Kokitsi Maninis, and Luc Van Gool. The 2019 davis challenge on vos: Unsupervised multi-object segmentation. *arXiv:1905.00737*, 2019. [1](#), [6](#)
- [7] Jiale Cao, Rao Muhammad Anwer, Hisham Cholakkal, Fahad Shahbaz Khan, Yanwei Pang, and Ling Shao. Sipmask: Spatial information preservation for fast image and video instance segmentation. In *Computer Vision—ECCV 2020: 16th European Conference, Glasgow, UK, August 23–28, 2020, Proceedings, Part XIV 16*, pages 1–18. Springer, 2020. [3](#), [8](#)
- [8] Nicolas Carion, Francisco Massa, Gabriel Synnaeve, Nicolas Usunier, Alexander Kirillov, and Sergey Zagoruyko. End-to-end object detection with transformers. In *European conference on computer vision*, pages 213–229. Springer, 2020. [3](#)
- [9] Yuhua Chen, Jordi Pont-Tuset, Alberto Montes, and Luc Van Gool. Blazingly fast video object segmentation with pixel-wise metric learning. In *Proceedings of the IEEE conference on computer vision and pattern recognition*, pages 1189–1198, 2018. [3](#)
- [10] Bowen Cheng, Ishan Misra, Alexander G Schwing, Alexander Kirillov, and Rohit Girdhar. Masked-attention mask transformer for universal image segmentation. In *Proceedings of the IEEE/CVF Conference on Computer Vision and Pattern Recognition*, pages 1290–1299, 2022. [3](#), [7](#), [8](#)
- [11] Bowen Cheng, Alex Schwing, and Alexander Kirillov. Per-pixel classification is not all you need for semantic segmentation. *Advances in Neural Information Processing Systems*, 34:17864–17875, 2021. [3](#)
- [12] Ho Kei Cheng, Yu-Wing Tai, and Chi-Keung Tang. Rethinking space-time networks with improved memory coverage for efficient video object segmentation. *Advances in Neural Information Processing Systems*, 34, 2021. [3](#), [6](#), [8](#)
- [13] Jingchun Cheng, Yi-Hsuan Tsai, Shengjin Wang, and Ming-Hsuan Yang. Segflow: Joint learning for video object segmentation and optical flow. In *Proceedings of the IEEE international conference on computer vision*, pages 686–695, 2017. [3](#)
- [14] Achal Dave, Pavel Tokmakov, and Deva Ramanan. Towards segmenting anything that moves. In *Proceedings of the IEEE/CVF International Conference on Computer Vision Workshops*, pages 0–0, 2019. [3](#)
- [15] Bert De Brabandere, Davy Neven, and Luc Van Gool. Semantic instance segmentation with a discriminative loss function. *arXiv preprint arXiv:1708.02551*, 2017. [3](#)
- [16] Bin Dong, Fangao Zeng, Tiancai Wang, Xiangyu Zhang, and Yichen Wei. Solq: Segmenting objects by learning queries. *Advances in Neural Information Processing Systems*, 34:21898–21909, 2021. [3](#)
- [17] Katerina Fragkiadaki, Geng Zhang, and Jianbo Shi. Video segmentation by tracing discontinuities in a trajectory embedding. In *2012 IEEE Conference on Computer Vision and Pattern Recognition*, pages 1846–1853. IEEE, 2012. [3](#)
- [18] Shubhika Garg and Vidit Goel. Mask selection and propagation for unsupervised video object segmentation. In *Proceedings of the IEEE/CVF Winter Conference on Applications of Computer Vision*, pages 1680–1690, 2021. [3](#)
- [19] Vik Goel, Jameson Weng, and Pascal Poupart. Unsupervised video object segmentation for deep reinforcement learning. *arXiv preprint arXiv:1805.07780*, 2018. [7](#)
- [20] Su Ho Han, Sukjun Hwang, Seoung Wug Oh, Yeonchool Park, Hyunwoo Kim, Min-Jung Kim, and Seon Joo Kim. Visolo: Grid-based space-time aggregation for efficient online video instance segmentation. In *Proceedings of the IEEE/CVF Conference on Computer Vision and Pattern Recognition*, pages 2896–2905, 2022. [3](#)
- [21] Kaiming He, Georgia Gkioxari, Piotr Dollár, and Ross Girshick. Mask r-cnn. In *Proceedings of the IEEE international conference on computer vision*, pages 2961–2969, 2017. [1](#), [3](#)
- [22] Zhaojin Huang, Lichao Huang, Yongchao Gong, Chang Huang, and Xinggang Wang. Mask scoring r-cnn. In *Proceedings of the IEEE/CVF Conference on Computer Vision and Pattern Recognition*, pages 6409–6418, 2019. [3](#)
- [23] Sukjun Hwang, Miran Heo, Seoung Wug Oh, and Seon Joo Kim. Video instance segmentation using inter-frame communication transformers. *Advances in Neural Information Processing Systems*, 34:13352–13363, 2021. [3](#)

- [24] Fuxin Li, Taeyoung Kim, Ahmad Humayun, David Tsai, and James M Rehg. Video segmentation by tracking many figure-ground segments. In *Proceedings of the IEEE International Conference on Computer Vision*, pages 2192–2199, 2013. 3
- [25] Yu Li, Zhuoran Shen, and Ying Shan. Fast video object segmentation using the global context module. In *European Conference on Computer Vision*, pages 735–750. Springer, 2020. 3
- [26] Huaijia Lin, Ruizheng Wu, Shu Liu, Jiangbo Lu, and Jiaya Jia. Video instance segmentation with a propose-reduce paradigm. In *Proceedings of the IEEE/CVF International Conference on Computer Vision (ICCV)*, pages 1739–1748, October 2021. 2, 3, 4, 5, 6, 7, 8
- [27] Tsung-Yi Lin, Michael Maire, Serge Belongie, James Hays, Pietro Perona, Deva Ramanan, Piotr Dollár, and C Lawrence Zitnick. Microsoft coco: Common objects in context. In *European conference on computer vision*, pages 740–755. Springer, 2014. 7
- [28] Shu Liu, Jiaya Jia, Sanja Fidler, and Raquel Urtasun. Sgn: Sequential grouping networks for instance segmentation. In *Proceedings of the IEEE International Conference on Computer Vision*, pages 3496–3504, 2017. 3
- [29] Shu Liu, Lu Qi, Haifang Qin, Jianping Shi, and Jiaya Jia. Path aggregation network for instance segmentation. In *Proceedings of the IEEE conference on computer vision and pattern recognition*, pages 8759–8768, 2018. 3
- [30] Xiankai Lu, Wenguan Wang, Chao Ma, Jianbing Shen, Ling Shao, and Fatih Porikli. See more, know more: Unsupervised video object segmentation with co-attention siamese networks. In *The IEEE Conference on Computer Vision and Pattern Recognition (CVPR)*, 2019. 3
- [31] Jonathon Luiten, Idil Esen Zulfikar, and Bastian Leibe. Unovost: Unsupervised offline video object segmentation and tracking. In *Proceedings of the IEEE/CVF Winter Conference on Applications of Computer Vision*, pages 2000–2009, 2020. 1, 3, 6, 7
- [32] Alejandro Newell, Zhiao Huang, and Jia Deng. Associative embedding: End-to-end learning for joint detection and grouping. *arXiv preprint arXiv:1611.05424*, 2016. 3
- [33] Hung Nguyen and Fuxin Li. Space time recurrent memory network. *arXiv preprint arXiv:2109.06474*, 2021. 3
- [34] Seoung Wug Oh, Joon-Young Lee, Kalyan Sunkavalli, and Seon Joo Kim. Fast video object segmentation by reference-guided mask propagation. In *The IEEE Conference on Computer Vision and Pattern Recognition (CVPR)*, 2018. 3
- [35] Seoung Wug Oh, Joon-Young Lee, Ning Xu, and Seon Joo Kim. Video object segmentation using space-time memory networks. In *Proceedings of the IEEE/CVF International Conference on Computer Vision (ICCV)*, October 2019. 1, 3, 6, 7
- [36] Federico Perazzi, Anna Khoreva, Rodrigo Benenson, Bernt Schiele, and Alexander Sorkine-Hornung. Learning video object segmentation from static images. In *Proceedings of the IEEE conference on computer vision and pattern recognition*, pages 2663–2672, 2017. 3
- [37] Federico Perazzi, Jordi Pont-Tuset, Brian McWilliams, Luc Van Gool, Markus Gross, and Alexander Sorkine-Hornung. A benchmark dataset and evaluation methodology for video object segmentation. In *Proceedings of the IEEE conference on computer vision and pattern recognition*, pages 724–732, 2016. 6
- [38] Jordi Pont-Tuset, Federico Perazzi, Sergi Caelles, Pablo Arbeláez, Alex Sorkine-Hornung, and Luc Van Gool. The 2017 davis challenge on video object segmentation. *arXiv preprint arXiv:1704.00675*, 2017. 6
- [39] Hongje Seong, Junhyuk Hyun, and Euntai Kim. Kernelized memory network for video object segmentation. In *European Conference on Computer Vision*, pages 629–645. Springer, 2020. 3
- [40] Hongmei Song, Wenguan Wang, Sanyuan Zhao, Jianbing Shen, and Kin-Man Lam. Pyramid dilated deeper convlstm for video salient object detection. In *Proceedings of the European conference on computer vision (ECCV)*, pages 715–731, 2018. 6, 7
- [41] Omkar Thawakar, Sanath Narayan, Jiale Cao, Hisham Cholakkal, Rao Muhammad Anwer, Muhammad Haris Khan, Salman Khan, Michael Felsberg, and Fahad Shahbaz Khan. Video instance segmentation via multi-scale spatio-temporal split attention transformer. *arXiv preprint arXiv:2203.13253*, 2022. 3
- [42] Omkar Thawakar, Sanath Narayan, Jiale Cao, Hisham Cholakkal, Rao Muhammad Anwer, Muhammad Haris Khan, Salman Khan, Michael Felsberg, and Fahad Shahbaz Khan. Video instance segmentation via multi-scale spatio-temporal split attention transformer. *Proc. European Conference on Computer Vision (ECCV)*, 2022. 3
- [43] Pavel Tokmakov, Karteek Alahari, and Cordelia Schmid. Learning motion patterns in videos. In *Proceedings of the IEEE conference on computer vision and pattern recognition*, pages 3386–3394, 2017. 3
- [44] Carles Ventura, Miriam Bellver, Andreu Girbau, Amaia Salvador, Ferran Marques, and Xavier Giro-i Nieto. Rvos: End-to-end recurrent network for video object segmentation. In *The IEEE Conference on Computer Vision and Pattern Recognition (CVPR)*, June 2019. 3, 6, 7
- [45] Paul Voigtlaender, Yuning Chai, Florian Schroff, Hartwig Adam, Bastian Leibe, and Liang-Chieh Chen. Feelvos: Fast end-to-end embedding learning for video object segmentation. In *Proceedings of the IEEE/CVF Conference on Computer Vision and Pattern Recognition*, pages 9481–9490, 2019. 3
- [46] Huiyu Wang, Yukun Zhu, Hartwig Adam, Alan Yuille, and Liang-Chieh Chen. Max-deeplab: End-to-end panoptic segmentation with mask transformers. In *Proceedings of the IEEE/CVF conference on computer vision and pattern recognition*, pages 5463–5474, 2021. 3
- [47] Tao Wang, Ning Xu, Kean Chen, and Weiyao Lin. End-to-end video instance segmentation via spatial-temporal graph neural networks. In *Proceedings of the IEEE/CVF International Conference on Computer Vision*, pages 10797–10806, 2021. 3
- [48] Wenguan Wang, Xiankai Lu, Jianbing Shen, David J. Crandall, and Ling Shao. Zero-shot video object segmentation via attentive graph neural networks. In *The IEEE International Conference on Computer Vision (ICCV)*, 2019. 3, 6, 7

[49] Wenguan Wang, Jianbing Shen, Xiankai Lu, Steven CH Hoi, and Haibin Ling. Paying attention to video object pattern understanding. *IEEE transactions on pattern analysis and machine intelligence*, 2020. 6, 7

[50] Xinlong Wang, Tao Kong, Chunhua Shen, Yuning Jiang, and Lei Li. Solo: Segmenting objects by locations. In *European Conference on Computer Vision*, pages 649–665. Springer, 2020. 3

[51] Xinlong Wang, Rufeng Zhang, Tao Kong, Lei Li, and Chunhua Shen. Solov2: Dynamic and fast instance segmentation. *Proc. Advances in Neural Information Processing Systems (NeurIPS)*, 2020. 3, 6

[52] Yuqing Wang, Zhaoliang Xu, Xinlong Wang, Chunhua Shen, Baoshan Cheng, Hao Shen, and Huaxia Xia. End-to-end video instance segmentation with transformers. In *Proceedings of the IEEE/CVF Conference on Computer Vision and Pattern Recognition*, pages 8741–8750, 2021. 3

[53] Junfeng Wu, Yi Jiang, Song Bai, Wenqing Zhang, and Xiang Bai. Seqformer: Sequential transformer for video instance segmentation. In *European Conference on Computer Vision*, pages 553–569. Springer, 2022. 3, 7, 8

[54] Jialian Wu, Sudhir Yarram, Hui Liang, Tian Lan, Junsong Yuan, Jayan Eledath, and Gerard Medioni. Efficient video instance segmentation via tracklet query and proposal. In *Proceedings of the IEEE/CVF Conference on Computer Vision and Pattern Recognition*, pages 959–968, 2022. 3

[55] Ruizheng Wu, Huaijia Lin, Xiaojuan Qi, and Jiaya Jia. Memory selection network for video propagation. In *European Conference on Computer Vision*, pages 175–190. Springer, 2020. 3

[56] Zhengyang Wu, Fuxin Li, Rahul Sukthankar, and James M Rehg. Robust video segment proposals with painless occlusion handling. In *Proceedings of the IEEE Conference on Computer Vision and Pattern Recognition*, pages 4194–4203, 2015. 3

[57] Christopher Xie, Yu Xiang, Zaid Harchaoui, and Dieter Fox. Object discovery in videos as foreground motion clustering. In *Proceedings of the IEEE/CVF Conference on Computer Vision and Pattern Recognition*, pages 9994–10003, 2019. 3

[58] Enze Xie, Peize Sun, Xiaoge Song, Wenhai Wang, Xuebo Liu, Ding Liang, Chunhua Shen, and Ping Luo. Polarmask: Single shot instance segmentation with polar representation. In *Proceedings of the IEEE/CVF conference on computer vision and pattern recognition*, pages 12193–12202, 2020. 3

[59] Linjie Yang, Yuchen Fan, and Ning Xu. Video instance segmentation. In *Proceedings of the IEEE/CVF International Conference on Computer Vision*, pages 5188–5197, 2019. 3, 7

[60] Linjie Yang, Yanran Wang, Xuehan Xiong, Jianchao Yang, and Aggelos K Katsaggelos. Efficient video object segmentation via network modulation. In *Proceedings of the IEEE Conference on Computer Vision and Pattern Recognition*, pages 6499–6507, 2018. 3

[61] Jialin Yuan, Chao Chen, and Li Fuxin. Deep variational instance segmentation. *arXiv preprint arXiv:2007.11576*, 2020. 3

[62] Tianfei Zhou, Jianwu Li, Xueyi Li, and Ling Shao. Target-aware object discovery and association for unsupervised

video multi-object segmentation. In *Proceedings of the IEEE/CVF Conference on Computer Vision and Pattern Recognition (CVPR)*, pages 6985–6994, June 2021. 3, 6, 7, 8

[63] Tianfei Zhou, Shunzhou Wang, Yi Zhou, Yazhou Yao, Jianwu Li, and Ling Shao. Motion-attentive transition for zero-shot video object segmentation. In *Proceedings of the 34th AAAI Conference on Artificial Intelligence (AAAI)*, pages 13066–13073, 2020. 3, 6, 7

Supplementary Materials:

A. Additional Run-time Analysis. The results in Table 6 are generated by using an NVIDIA Tesla V100 GPU. We report the detailed run-time of each module in MCMPG. It shows that our MCMPG framework is very lightweight and takes minimal time to run. In the same Table, we also show how the run-time changes as we increase the number of key frames. As mentioned in the main paper, with the STCN-style encoder, the tracker does not need to re-compute features from the backbone network for each track, making the proposed approach much faster compared to the case when the STM-style encoder was utilized. Also, in the case of STCN, the total run-time scales better with an increasing number of key frames. In Table 6, we show the running time with STCN, which is at least $2.2\times$ faster even with 1 key frame and more than $3.0\times$ faster than with STM with more key frames.

Table 6. Run-time of MCMPG on DAVIS-UVOS 2017 *val* with 1, 2, and 4 key frames. While our framework is lightweight, when using STM the speed suffers since STM requires re-running the backbone for each proposal. Alternatively, one could use newer tracking algorithms such as STCN where all the proposals can share the same backbone features, which would make the system much faster

Module	1 key frame	2 key frames	4 key frames
Candidate Generation	7.50	14.60	29.52
Propagate to the key frame	0.09	0.13	0.25
MP-Graph	14.10	16.40	22.91
Multi-Object tracking with STM	475.60	971.10	1817.41
Sequential NMS	61.20	65.00	71.77
Total time with STM	544.39	1,066.83	1941.86
Multi-Object tracking with STCN	182.51	261.93	378.63
Total time with STCN	251.29 (2.2x faster)	357.66 (3.0x faster)	503.02 (3.9x faster)

B. Qualitative results

DAVIS 2017 *val*. In Fig. 5, we show the qualitative segmentation results of our approach on DAVIS-UVOS. The segmentation results are

overlayed on the input RGB sequence where different colors are used to indicate different object instances.

DAVIS 2019 *test-dev*. Some qualitative segmentation results of our approach on DAVIS-UVOS 2019 *test-dev* are shown in Fig.6.

YouTube-VIS 2019 *val*. Some qualitative segmentation results of our approach on YouTube-VIS 2019 *val* are shown in Fig.7.



Figure 5. : Qualitative results on three sequences from the DAVIS 2017 *val* set. We show frames that are sampled from challenging scenarios such as fast motion, background clutter, occlusions, and multi-object interaction

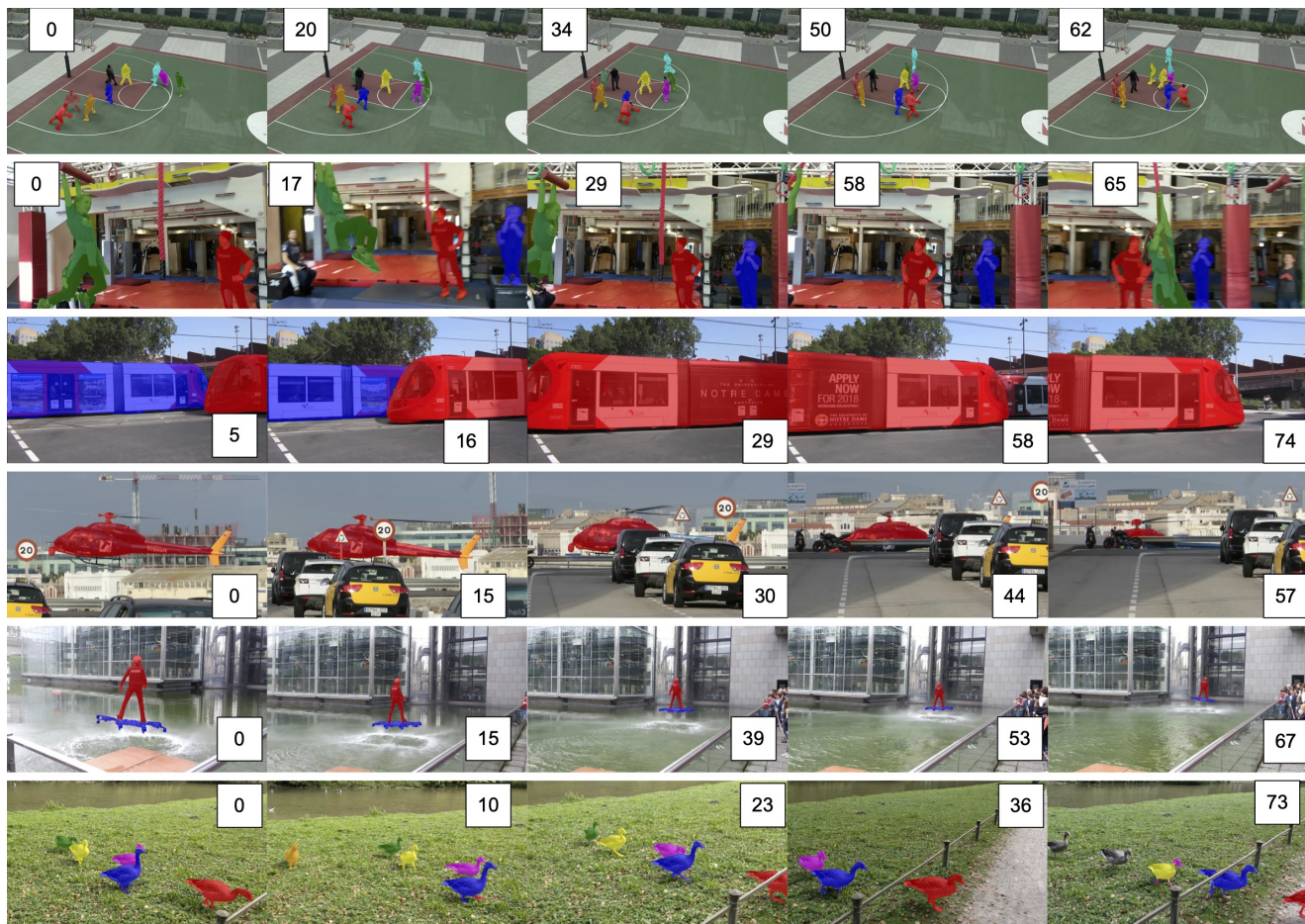


Figure 6. Qualitative results on sequences from DAVIS 2019 *test-dev*

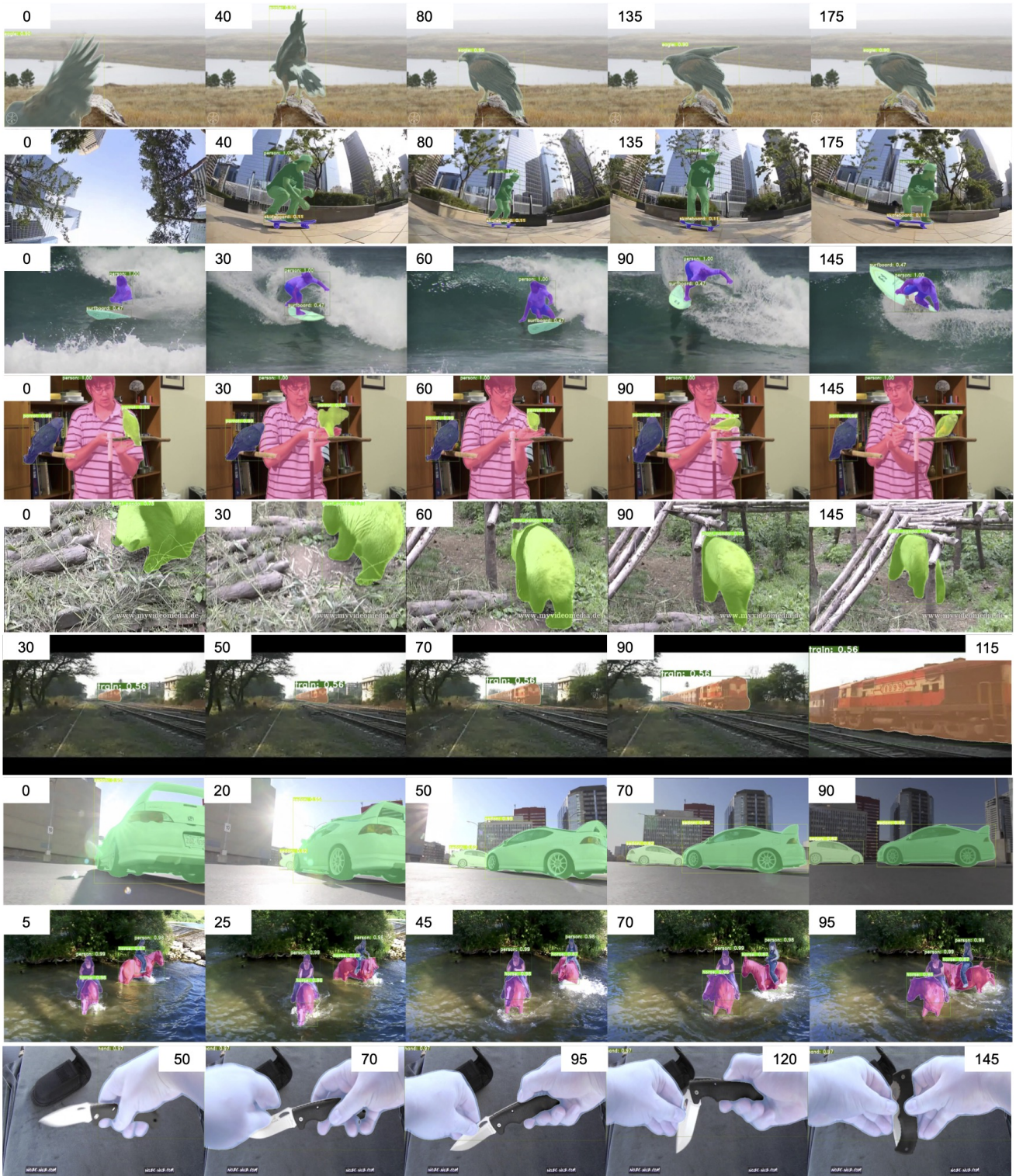


Figure 7. Qualitative results on sequences from YouTube-VIS 2019 *val*